Lu, C., Ward, A., Bettridge, J., Liu, Y. and Desiderio, S., An autoregulatory mechanism imposes epigenetic control on the V(D)J recombinase
Supplemental information

Supplemental data

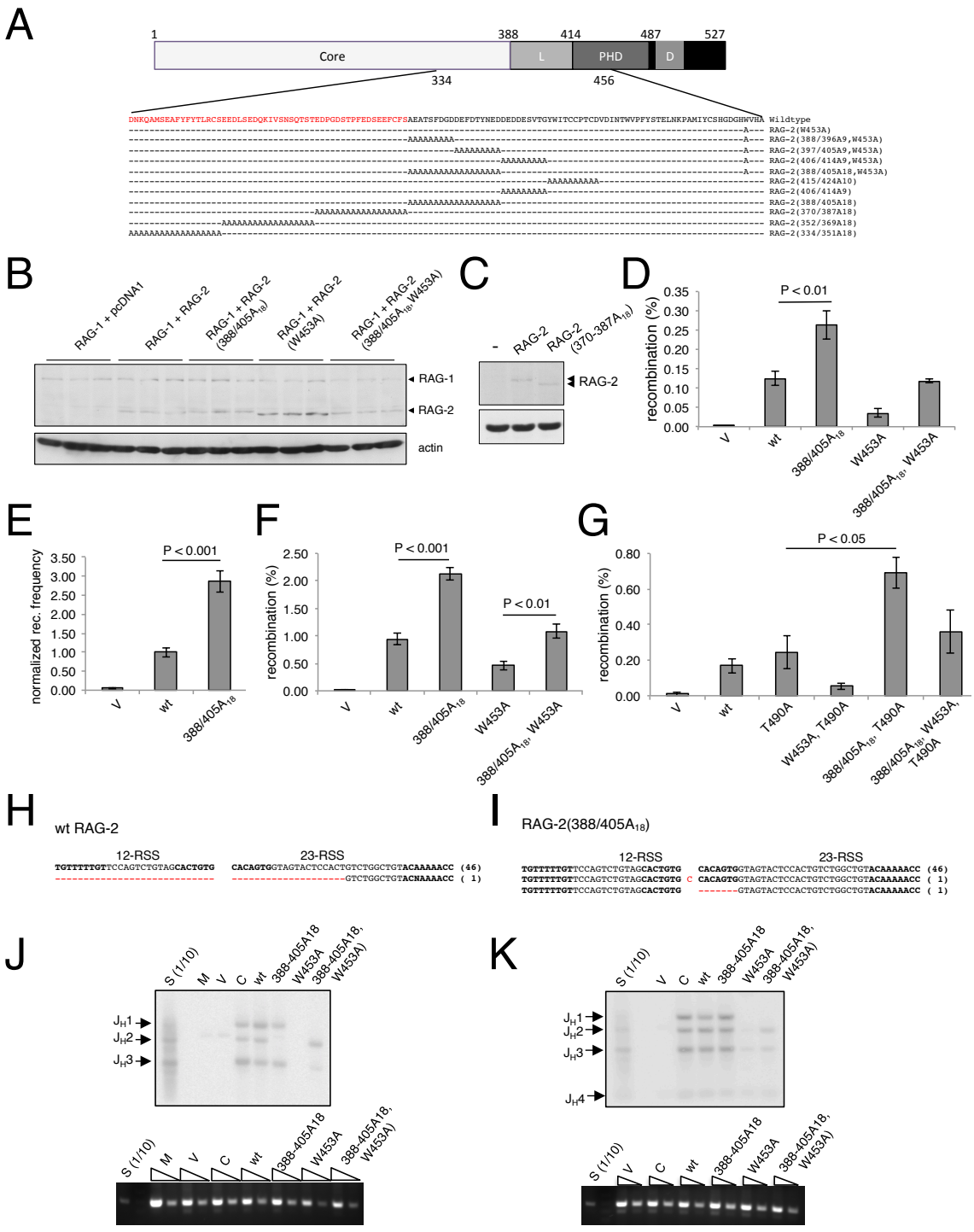

Figure S1. Mutation of the RAG-2 autoinhibitory domain is not associated with overexpression or aberrant signal joining. Related to Figure 1. (A) RAG-2 mutants. Above, diagram of RAG-2. Core, canonical core region; L, PHD and D, canonical linker region, plant homeodomain finger and signal for cell cycle-dependent degradation, respectively. Initial and terminal amino acid residues as well as residues bounding the core, linker and PHD finger are numbered. Below, amino acid sequences of wild-type RAG-2 and RAG-2 mutants in the interval from residues 334 through 456. Red type indicates residues residing in the canonical core region. Hyphens indicate identity to wild-type. (B) Immunodetection of RAG fusion proteins in recombination assays. NIH3T3 cells were cotransfected in triplicate with pJH200, RAG-1 and vector (pcDNA1), wild-type RAG-2, RAG-2(388/405A$_{18}$), RAG-2(W453A) or RAG-2(388/405A$_{18}$, W453A). An aliquot of cells from each transfection was lysed and RAG proteins (upper panel) or actin (lower panel) were detected by immunoblotting with an anti-myc or anti-actin antibody, respectively. Positions of RAG-1 and RAG-2 fusion proteins are indicated.
(C) Immunodetection of RAG-2(370/387A$_{18}$) and wild-type RAG-2 in transfected NIH3T3 cells. RAG-2 (upper panel) or actin (lower panel) were detected by immunoblotting as in (B). (D) Replicate assays confirm that the RAG-2 388/405A$_{18}$ mutation confers a robust gain-of-function phenotype. Recombination (%), frequency of signal joining in cells transfected with the extrachromosomal substrate pJH200 (Hesse et al., 1987), full-length RAG-1 and vector (V), full-length wild-type RAG-2 (wt) or full-length RAG-2 mutants as indicated (mean ± S.E.M., n = 3 independent biological replicates, assessed on a different day and with a different passage of NIH3T3 cells from all other experiments presented). Statistical significance was determined by ANOVA. (E) Composite data from three independent signal joining assays, demonstrating the stimulatory effect of the 388/405A$_{18}$ mutation. Recombination frequency data from (D), Fig. 1A and Fig. 1B were normalized to wild-type. Assays of full-length RAG-1 in combination with vector (V), full-length wild-type RAG-2 (wt) or full-length RAG-2(388/405A$_{18}$) are indicated (mean ± S.E.M., n = 9 independent biological replicates, assessed on three different days). Statistical significance was determined by ANOVA. (F) The RAG-2 388/405A$_{18}$ mutation stimulates recombination and rescues a PHD domain mutant in an assay for coding joining. Recombination (%), frequency of coding joining in cells transfected with the extrachromosomal substrate pJH290 (Hesse et al., 1987), full-length RAG-1 and vector (V), full-length wild-type RAG-2 (wt) or full-length RAG-2 mutants as indicated [mean ± S.E.M., n = 3 independent biological replicates, assessed on a different day and with a different passage of NIH3T3 cells than all other experiments presented]. Statistical significance was determined by ANOVA. (G) The RAG-2 388/405A$_{18}$ mutation stimulates signal joining independent of cell cycle-dependent regulation of RAG activity. Recombination (%), frequency of signal joining in cells transfected with the extrachromosomal substrate pJH200 (Hesse et al., 1987), full-length RAG-1 and vector (V), full-length wild-type RAG-2 (wt) or full-length RAG-2 mutants as indicated (mean ± S.E.M., n = 3 independent biological replicates). The RAG-2 T490A mutation uncouples RAG activity from the cell cycle. Statistical significance was determined by ANOVA. (H) and (I) Signal joints obtained from

extrachromosomal assays with (H) wild-type RAG-2 or (I) RAG-2(388/405A_{18}). Nonamer and heptamer sequences associated with 12-RSS and 23-RSS substrates are indicated in boldface type; the numbers of clones represented by each sequence are indicated at right. Insertions and deletions are indicated in red type. (J) and (K) Replicate assays confirm that the 388/405A_{18} mutation reverses the debilitating effect of the W453A mutation on endogenous V(D)J recombination. Upper panels, assay for D_{SP2}-to-J_H joints in genomic DNA from uninfected cells (Un) or cells transduced with the following: vector alone (V), core RAG-2 (C), full-length wild-type RAG-2 (wt) or full-length RAG-2 mutants as indicated at top. (S), splenic genomic DNA; (M), mock transduction. Positions of D_{SP2}-to-J_H recombinants are indicated at left. Lower panels, control for input genomic DNA, as assessed by amplification of the RAG-1 locus by PCR.

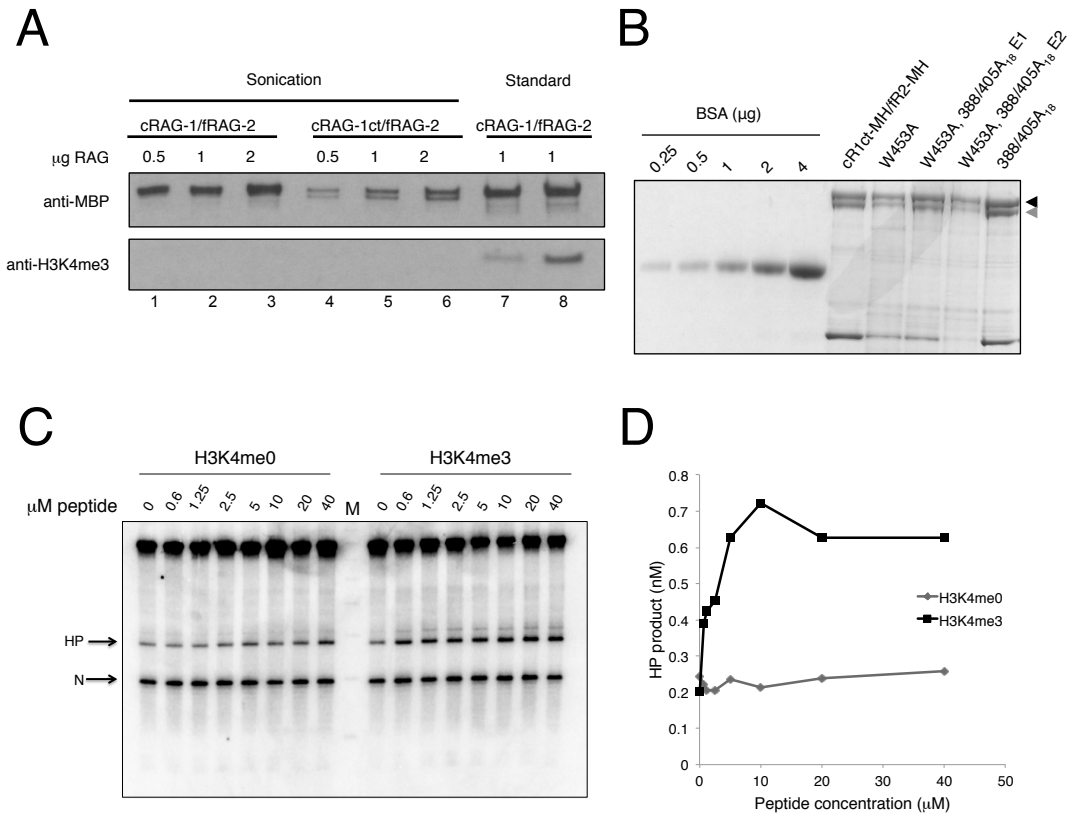

Figure S2. Stimulation of H3K4me3-depleted wild-type RAG by exogenous H3K4me3. Related to Figure 1. (A) Separation of RAG from endogenous H3K4me3. Detection of RAG proteins (upper panel) or H3K4me3 (lower panel) by immunoblotting with anti-myc or anti-H3K4me3 antibody, respectively. The RAG fusion proteins cRAG-1-MH (cRAG-1) and fRAG-2-MH (fRAG-2) (lanes 1 – 3, lane 7 and lane 8) or cRAG-1ct-MH (cRAG-1ct) and fRAG-2-MH (lanes 4 – 6), as defined in Fig. 1, were expressed in HEK-293T cells. RAG complexes were purified by a standard procedure (lanes 7 and 8) or by a protocol that included sonication prior to affinity chromatography (lanes 1 – 6). The amounts of total RAG protein loaded are indicated in μg. (B) Complexes of cRAG-1ct-MH (cR1ct-MH) with fRAG-2-MH (fR2-MH) or the indicated single or double full-length RAG-2 mutants were purified by sonication and amylose affinity chromatography. Aliquots of each preparation were fractionated by SDS-PAGE alongside a dilution series of bovine serum albumin (BSA). E1 and E2 designate sequential amylose eluates. The positions of the RAG-1 and RAG-2 fusion proteins are indicated by black and gray arrowheads, respectively. (C) Coupled cleavage reactions contained radiolabeled 23-RSS and unlabeled 12-RSS. Additions of RAG and H3K4me0 or H3K4me3 are indicated above. The positions of hairpin (HP) and nicked (N) products are indicated by arrows. M, 10 bp marker ladder. (D) Accumulation of hairpin product (percent of total substrate) at 1 hr is plotted as a function of the concentration of H3K4me0 (gray diamonds) or H3K4me3 (black squares).

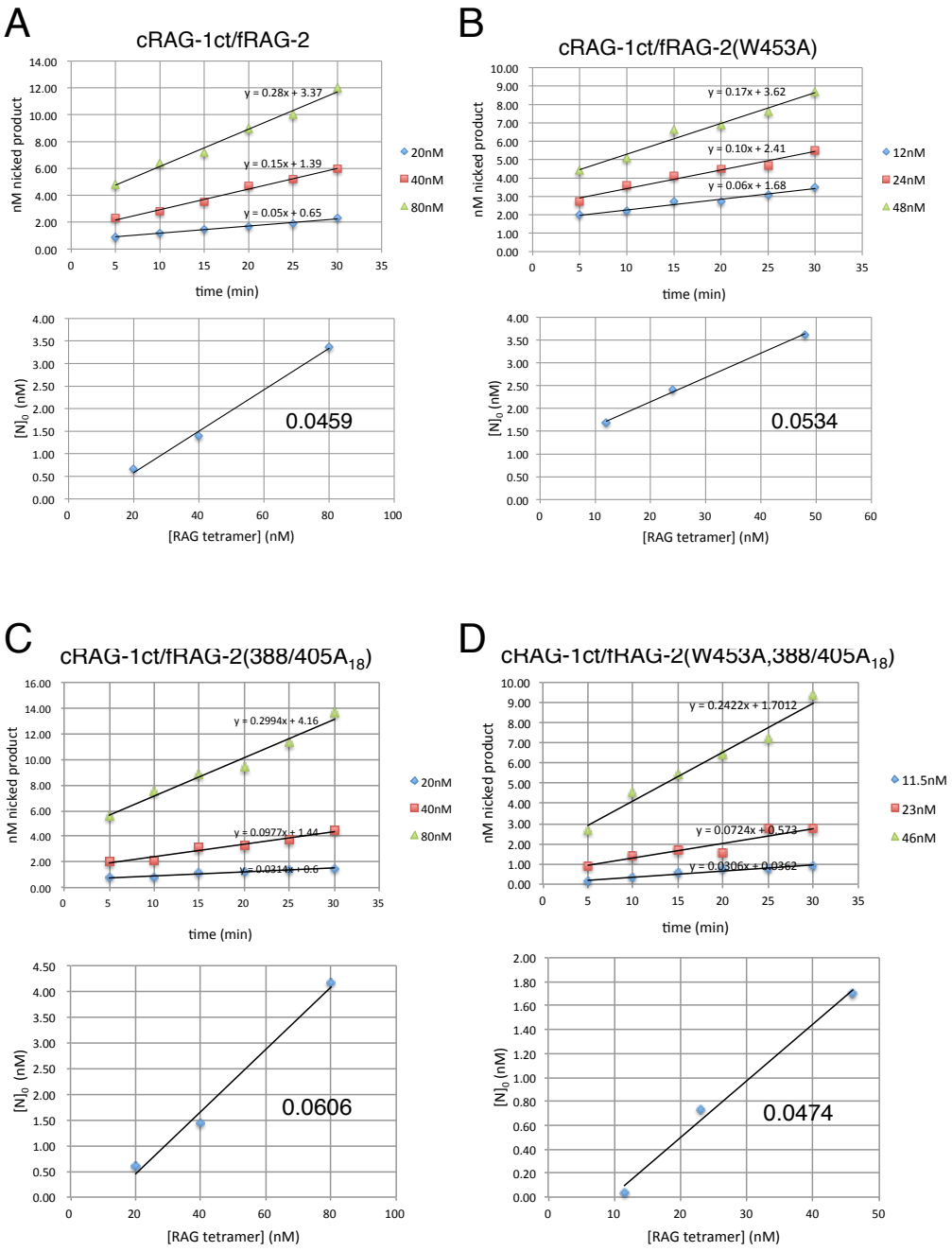

Figure S3. Burst kinetic analysis of wild-type and mutant RAG complexes. Related to Figures 2 and 3. Complexes of cRAG-1ct-MH (cRAG-1ct) with (A) full-length wild-type RAG-2-MH (fRAG-2) or the corresponding (B) W453A, (C) 388/405A$_{18}$ and (D) W453A, 388/405A$_{18}$ RAG-2 mutants were assayed for nicking of a 12-RSS substrate at various nominal RAG concentrations. Upper panels, accumulation of nicked product as a function of time; nominal RAG concentation, calculated on the basis of tetrameric stoichiometry, is indicated at right. Lower panels, estimation of active fraction. The

kinetic curves of the upper panels were extrapolated to zero time to give the $[N]_0$ associated with each nominal RAG concentration ([RAG tetramer]). $[N]_0$ was then plotted as a function of ([RAG tetramer]; the slope of each resulting curve represents the fraction of active RAG in the preparation. The active fractions of the four preparations were similar, ranging from 4.6 percent to 6.1 percent.

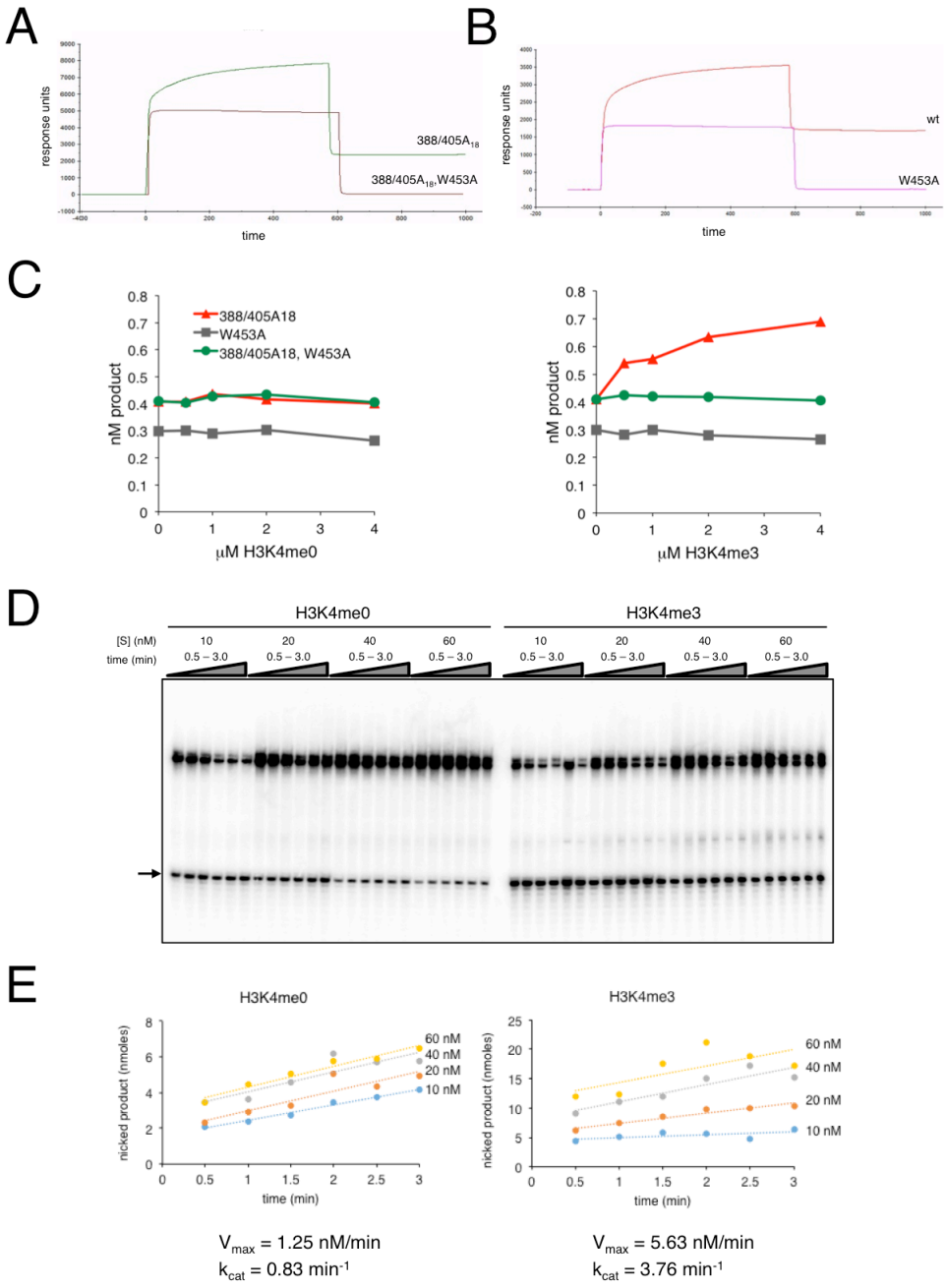

Figure S4. Stimulatory effects of the 388/405A$_{18}$ mutation and exogenous H3K4me3 on in vitro nicking by H3K4me3-depleted RAG. Related to Figures 2 and 4. (A) and (B) Surface plasmon resonance assays for association of RAG-2 constructs with a histone H3K4me3 peptide. Biotin-tagged H3K4me3 peptide (residues 1 – 21) was immobilized at 24 pmol on biosensor chips. GST-tagged RAG-2$_{PHD}$, RAG-2$_{PHD}$(W453A), RAG-2$_{PHD}$(388/405A$_{18}$) or RAG-2$_{PHD}$(388/405A$_{18}$, W453A) were brought to 2 μM and injected 10 min at a flow rate of 5 μl/min; this was followed by injection of running buffer alone

for 10 min. (A) Comparison of RAG-2_{PHD}(388/405A_{18}) and RAG-2_{PHD}(388/405A_{18}, W453A). (B) Comparison of wild-type RAG-2_{PHD} and RAG-2_{PHD}(W453A). (C) The 388/405A_{18} mutation enhances in vitro nicking activity of full length RAG-2(W453A) in complex with full-length RAG-1. Complexes of flR1-MH and full-length RAG-2(388/405A_{18}), RAG-2(W453A) or RAG-2(388/405A_{18}, W453A) were purified under conditions that removed endogenous H3K4me3. Activities were normalized by burst kinetics and equivalent amounts of active tetramer were assayed for nicking of a 12-RSS substrate. Accumulation of nicked product at 30 min (nM product) is plotted as a function of the concentration of H3K4me0 (left) or H3K4me3 (right). Gray squares, RAG-2(W453A); red triangles, RAG-2(388/405A_{18}); green circles, RAG-2(388/405A_{18}, W453A). Data are representative of two experiments. (D) Assay for RSS nicking. Reactions contained 1.5 nM fRAG-2-MH and 12-RSS substrate HL44/45 at 10, 20, 40 or 60 nM. Reactions were supplemented with 4 μM H3K4me0 or H3K4me3 peptide as indicated at top. Accumulation of nicked product (arrow) was assayed at times ranging from 0.5 min to 3 min. (E) Concentration of nicked product as determined in (D) is plotted as a function of time for each substrate concentration. Blue, 10 nM; orange, 20 nM; gray, 40 nM; and yellow, 60 nM. Left, reactions containing H3K4me0; right, reactions containing H3K4me3. V_{max} was determined from the slopes of the individual kinetic curves by non-linear regression analysis as described in Experimental Procedures; $k_{cat} = V_{max}/[RAG]_T$, where $[RAG]_T$ is the total concentration of active RAG tetramer.

Table S1.

	RAG-2		RAG-2(388/405A$_{18}$)	
	+ H3K4me0	**+H3K4me3**	**+ H3K4me0**	**+H3K4me3**
K_D	242 nM	76 nM	88 nM	84 nM
k_{cat}	0.83 min^{-1}	3.76 min^{-1}	4.95 min^{-1}	7.06 min^{-1}

Table S1. Estimates of dissociation constants (K_D) and catalytic rate (k_{cat}) for full-length wild-type RAG-2 and full-length RAG-2(388/405A$_{18}$) in complex with cR1ct-MH. Related to Figures 3 and 4. K_D was measured for a canonical 12-RSS substrate; k_{cat} was determined in an assay for nicking of a 12-RSS substrate.

Supplemental experimental procedures

Expression constructs

Plasmids pcRAG-2 (Ross et al., 2003), encoding full length RAG-2, and plasmids encoding maltose-binding protein (MBP) fusions to full-length RAG-1, core RAG-1 or full-length RAG-2, tagged at the c-termini with a myc epitope and polyhistidine, have been described (Jiang et al., 2004; McBlane et al., 1995). To construct a plasmid expressing core RAG-1ct (Grundy et al., 2010), codons 384 through 1040 of mouse RAG-1 were amplified by PCR and ligated in frame between cassettes encoding MBP and myc-polyhistidine that had been inserted into the vector pcDNA3.1. Mutations encoding clustered alanine substitutions were introduced into pcRAG-2 by divergent PCR using the following primer pairs:

Mutation	Primer (5'-3')
(334/351)A_{18}	5'GCCGCTGCAGCTGCTGCTGCTGCTGCTGCTGCTGCTGAAGAGGATTTGAGTGAAG3'
	5'GCCGCTGCAGCGGCGGCGGCGGCGGCGGCGGCTCCTGGTATGCCAAGG3'
(352/369)A_{18}	5'GCCGCTGCAGCTGCTGCTGCTGCTGCTGCTGCTGCTGAAGATCCTGGGGACTC3'
	5'GCCGCTGCAGCGGCGGCGGCGGCGGCGGCGGCAGAGCATCTCAAAGTATAG3'
(370/387)A_{18}	5'GCCGCTGCAGCTGCTGCTGCTGCTGCTGCTGCTGCTGCTGAAGCAACCAGTTTTG3'
	5'GCCGCTGCAGCGGCGGCGGCGGCGGCGGCGGCTGTTGATGTCTGACTGTTG3'
(388-396)A_{9}	5'GCCGCTGCAGCTGCTGCTGCTGATGAATTTGACACCTAC3'
	5'GCCGCTGCAGCGGCGGCGGCACTGAAACAAAATTCCTC3'

(397-405)A_9	5'GCCGCTGCAGCTGCTGCTGCTGATGAAGATGACGAGTC3'
	5'GCCGCTGCAGCGGCGGCGGCGTCACCATCAAAACTGG3'
(388-405)A_{18}	5'GCCGCTGCAGCTGCTGCTGCTGCTGCTGCTGCTGATGAAGATGACGAGTC3'
	5'GCCGCTGCAGCGGCGGCGGCGGCGGCGGCACTGAAACAAAATTCCTC3'
(406-414)A_9	5'GCCGCTGCAGCTGCTGCTGCTTACTGGATAACATGTTGC3'
	5'GCCGCTGCAGCGGCGGCGGCATCTTCATTGTAGGTGTC3'
(415-424)A_{10}	5'GCCGCTGCAGCTGCTGCTGCTGTTGACATCAATACCTGG3'
	5'GCCGCTGCAGCGGCGGCGGCGCCGGTTACAGACTCGTC3'

Protein purification

Except where noted, all RAG proteins assayed in vitro were fused at the amino terminus to MBP and at the carboxyl terminus to a myc epitope and a polyhistidine tag. Core RAG-1 (cR1-MH), the core RAG-1ct variant (cR1ct-MH) or full-length RAG-1 (flR1-MH) were co-expressed in HEK 293T cells with full-length RAG-2 (fR2-MH) or the corresponding RAG-2 mutants. RAG complexes were purified as described (Raval et al., 2008). Transfected 293T cells were harvested in PBS-EDTA [1X PBS, 2mM EDTA] and pelleted at 500 g at 4°C for 5 minutes. The supernatant was aspirated and cell pellets were resuspended in 7ml buffer R [25 mM HEPES (pH 7.4), 150 mM KCl, 2 mM DTT, 1.04 mM aminoethyl-benzenesulfonyl fluoride, 0.8 μM aprotinin, 40 nM bestatin, 14 nM E-64, 20 nM leupeptin, 15 nM pepstatin A and 10% glycerol]. Cell suspensions were placed in a 50% ethanol dry ice bath and subjected to 3 rounds of sonication in a Branson Digital Sonifier 450. Each round of sonication was performed at 23% amplitude for 1.5

minutes, with 30 second intervals of sonication followed by a 10 second rest between intervals. The lysate was clarified by centrifugation at 46,000 g in an SW55Ti rotor at 4°C for 30 min and the supernatant was loaded onto 1 ml amylose resin that had been equilibrated with buffer R. The column was washed once with 5 ml buffer R and once with 5 ml buffer R lacking protease inhibitors. Protein was eluted with 10 mM maltose in buffer R lacking protease inhibitors and then dialyzed against buffer R. Aliquots were snap frozen and stored at -80˚C.

Extrachromosomal recombination assays

Extrachromosomal recombination assays were performed as described (Hesse et al., 1987) with slight modification. Briefly, plasmids (10 μg each) encoding MBP-RAG-1-myc-His and wild-type RAG-2 or a RAG-2 mutant were cotransfected with 4 μg pJH200 into NIH3T3 cells. After 48 hr plasmid was recovered from half of the cells ($4x10^6$) by alkaline lysis and the remaining half were lysed in RIPA buffer [20 mM Tris-HCl (pH 7.5), 150 mM NaCl, 1 mM Na_2EDTA, 1 mM EGTA, 1% NP-40, 1% sodium deoxycholate, 2.5 mM sodium pyrophosphate, 1 mM β-glycerophosphate, 1 mM Na_3VO_4, 1 μg/mL leupeptin, and 1 mM phenylmethanesulfonylfluoride] for assays of protein expression. *E. coli* DH5α was transformed with 2 μL (about 40 μg) plasmid DNA and 1.7% of each transformation mix was plated on LB agar containing 50 μg /ml ampicillin; the remainder was plated on LB agar containing 50 μg /ml ampicillin and 12.5 μg /ml chloramphenicol. Plates containing ampicillin alone were scored at 16 hr; plates containing ampicillin and chloramphenicol were scored after 20 hr at 37˚C. Within a

given experiment each RAG-2 variant was assayed in triplicate; each replicate involved an independent transfection of NIH3T3 cells.

Assay for endogenous D-to-J_H recombination

The retroviral vector pCLIP2A (Pomerantz et al., 2002) was engineered to coexpress puromycin N-acetyl transferase and RAG-2, RAG-2(388/405A_{18}), RAG-2(W453A), RAG-2(388/405A_{18}, W453A). Viral particles were used to infect *Rag-2*$^{-/-}$ 63-12 pro-B cells (5 x 10^5) by spin inoculation in the presence of 10 μg/ml polybrene. Infected cells were maintained under puromycin selection in RPMI-1640 medium supplemented with 10% FBS, 10 mM HEPES, 2 mM L-glutamine, 1 mM sodium pyruvate, 50 μM β-mercaptoethanol, 0.7x non-essential amino acids, 50 u/ml penicillin/streptomycin and 1 μg/ml puromycin. After 25 d genomic DNA and total cellular protein were harvested.

A PCR-based assay was used to detect endogenous D-to-J_H recombination. Genomic DNA from transduced cells (90 ng) was amplified using forward primers specific for DSP2 (5'-ATGGCCCCTGACACTCTGCACTGC T-3') and a reverse primer that initiates synthesis from a site 3' of J_H4 (5'-AAAGACCTGGAGAGGCCATTCT-TACC-3'). Amplification was performed using the following protocol: 1 cycle at 95˚C for 5 min; 33 cycles of 94˚C for 1 min, 65˚C for 1 min and 72˚C for 3 min; 1 cycle at 72˚C for 10 min. Products were detected by Southern hybridization to a degenerate oligonucleotide probe that recognizes all J_H segments (5'-CTYACCTGMRGAGAC-DGTGAS-3'). The genomic DNA samples were normalized for quality and quantity by

PCR amplification of the mouse *RAG-1* locus using primers 5'- GCATCTATTCTG-TAGGATCTGC-3' and 5'- AAACAATGTCAAGCAGACAGCC-3'.

Burst kinetic analysis

RAG protein was combined at varying nominal concentrations with 200 nM total radiolabeled HL44/45 in binding buffer containing 1% glycerol (reaction volume 10 μl) and incubated for 20 min at 37°C, at which time $MgCl_2$ was added to 5 mM. Incubation was continued for an additional 30 min at 37°C. Reactions were stopped by addition of 10 μl 90% formamide-TBE and heated for 5 min at 95°C. Products were fractioned by electrophoresis on a 15% polyacrylamide-urea gel, visualized by a phosphorimager quantified using ImageQuantNL. The active fraction of each RAG preparation was determined by (1) plotting accumlation of nicked product ([N]) as a function of time for each concentration of total RAG; (2) extrapolating rates to zero time, thereby obtaining the initial burst of nicked product formation ($[N]_0$) at each nominal RAG concentration; and (3) expressing $[N]_0$ as a linear function of nominal RAG concentration:

$$[N]_0 = f_a \cdot [RAG]_T + b$$

where $[RAG]_T$ is the total (nominal) concentration of RAG, assuming a tetrameric stoichiometry of $(RAG\text{-}1)_2(RAG\text{-}2)_2$, and f_a is the fraction of $[RAG]_T$ that is active (Yu and Lieber, 2000).

Assays for coupled cleavage

RAG (1 nM active tetramer, as determined by burst kinetic analysis) was combined in binding buffer with 5 nM HL44/45, 5nM HL46/47 and varying concentrations of a

peptide corresponding to the amino-terminal 21 residues of histone H3, either trimethylated at lysine 4 (H3K4me3; Anaspec, 64194) or unmethylated (H3K4me0; Anaspec, 61701), in a reaction volume of 10 μl. After incubation for 20 min at 37°C, $MgCl_2$ was added to 5 mM and incubation was continued for an additional 1 hr. Reactions were stopped and products were analyzed as above.

Assays for DNA nicking by full-length RAG proteins

Full length RAG (1 nM active tetramer, as determined by burst kinetic analysis) was combined in binding buffer with 5 nM HL44/45 and varying concentrations of a peptide corresponding to the amino-terminal 21 residues of histone H3, either trimethylated at lysine 4 (H3K4me3; Anaspec, 64194) or unmethylated (H3K4me0; Anaspec, 61701), in a reaction volume of 10 μl. After incubation for 20 min at 37°C, $MgCl_2$ was added to 5 mM and incubation was continued for an additional 30 min. Reactions were stopped and products were analyzed as above.

Surface plasmon resonance

Surface plasmon resonance assays were performed using a BIAcore 2000 biosensor at 25˚C. A biotinylated histone H3 peptide, trimethylated on lysine 4 (24 pmol), was immobilized on streptavidin-coated biosensor chips. Chips were washed at a flow rate of 5 μl/min for 10 min with running buffer [PBS pH 7.4, 0.05% Na azide, 0.005% Tween 20]. GST-tagged RAG-2_{PHD} (Liu et al., 2007) or the corresponding mutant fusion proteins RAG-2_{PHD}(W453A), RAG-2_{PHD}(388/405A_{18}) and RAG-2_{PHD}(388/405A_{18}, W453A) were brought to a concentration of 2 μM in running buffer and injected for 10

min at a flow rate of 5 μl/min; this was followed by injection of running buffer alone for 10 min.

Supplemental references

Grundy, G.J., Yang, W., and Gellert, M. (2010). Autoinhibition of DNA cleavage mediated by RAG1 and RAG2 is overcome by an epigenetic signal in V(D)J recombination. Proc Natl Acad Sci U S A *107*, 22487-22492.

Hesse, J.E., Lieber, M.R., Gellert, M., and Mizuuchi, K. (1987). Extrachromosomal DNA substrates in pre-B cells undergo inversion or deletion at immunoglobulin V-(D)-J joining signals. Cell *49*, 775-783.

Jiang, H., Ross, A.E., and Desiderio, S. (2004). Cell cycle-dependent accumulation in vivo of transposition-competent complexes between recombination signal ends and full-length RAG proteins. J Biol Chem *279*, 8478-8486.

Liu, Y., Subrahmanyam, R., Chakraborty, T., Sen, R., and Desiderio, S. (2007). A plant homeodomain in RAG-2 that binds hypermethylated lysine 4 of histone H3 is necessary for efficient antigen-receptor-gene rearrangement. Immunity *27*, 561-571.

McBlane, J.F., van Gent, D.C., Ramsden, D.A., Romeo, C., Cuomo, C.A., Gellert, M., and Oettinger, M.A. (1995). Cleavage at a V(D)J recombination signal requires only RAG1 and RAG2 proteins and occurs in two steps. Cell *83*, 387-395.

Pomerantz, J.L., Denny, E.M., and Baltimore, D. (2002). CARD11 mediates factor-specific activation of NF-kappaB by the T cell receptor complex. The EMBO journal *21*, 5184-5194.

Raval, P., Kriatchko, A.N., Kumar, S., and Swanson, P.C. (2008). Evidence for Ku70/Ku80 association with full-length RAG1. Nucleic Acids Res *36*, 2060-2072.

Ross, A.E., Vuica, M., and Desiderio, S. (2003). Overlapping signals for protein degradation and nuclear localization define a role for intrinsic RAG-2 nuclear uptake in dividing cells. Mol Cell Biol *23*, 5308-5319.

Yu, K., and Lieber, M.R. (2000). The nicking step in V(D)J recombination is independent of synapsis: implications for the immune repertoire. Mol Cell Biol *20*, 7914-7921.